



HAL
open science

Energy transfer between acoustic fields by dry frictional contacts for SHM: a lumped numerical analysis

Konstantinos Gryllias, Eric Chatelet, Francesco Massi, Emmanuel Moulin

► To cite this version:

Konstantinos Gryllias, Eric Chatelet, Francesco Massi, Emmanuel Moulin. Energy transfer between acoustic fields by dry frictional contacts for SHM: a lumped numerical analysis. The 26th International Conference on Noise and Vibration engineering, Sep 2014, Louvain, Belgium. hal-01569145

HAL Id: hal-01569145

<https://hal.science/hal-01569145v1>

Submitted on 26 Jul 2017

HAL is a multi-disciplinary open access archive for the deposit and dissemination of scientific research documents, whether they are published or not. The documents may come from teaching and research institutions in France or abroad, or from public or private research centers.

L'archive ouverte pluridisciplinaire **HAL**, est destinée au dépôt et à la diffusion de documents scientifiques de niveau recherche, publiés ou non, émanant des établissements d'enseignement et de recherche français ou étrangers, des laboratoires publics ou privés.

Public Domain

Energy transfer between acoustic fields by dry frictional contacts for SHM: a lumped numerical analysis

K. C. Gryllias¹, E. Chatelet¹, Fr. Massi², E. Moulin³

¹LaMCoS UMR5259, CNRS, INSA-Lyon, University of Lyon, France

e-mail: konstantinos.gryllias@insa-lyon.fr

²Dipartimento di Ingegneria Meccanica e Aerospaziale, University of Rome "La Sapienza", Italy

³Department of OAE, IEMN, UMR CNRS 8520, Université de Valenciennes et du Hainaut Cambrésis, France

Abstract

This paper investigates the concept of transferring / pumping vibroacoustic energy from an ambient acoustic field towards a secondary acoustic field by exploiting the dry contact friction nonlinearities. The secondary acoustic field could be used, for instance, as a reference signal in structural health monitoring with various applications e.g. in aeronautics. Firstly the concept of energy dissipation by dry friction is examined for a nonlinear model of a simplified spring-mass-damper-dry friction damper system. A Masing macroslip contact model is introduced. The dynamic behavior of the system is calculated using a combination of a nonlinear Newmark method and a Newton-Raphson iterative method. The three different contact states (stick, stick/slip and slip) and peak flattening are observed. The analysis is further extended to a more complex system constituted by 3 degrees of freedoms and a frictional slider. The vibrational energy transfer between the different natural frequencies of the system and the exploitation of the ambient vibrational field are both investigated and demonstrated in numerical simulation results.

1 Introduction

Structural Health Monitoring (SHM) is an ensemble of emerging technologies focusing towards the improvement of the safety, the reliability and the maintainability of critical structures such as bridges, dams, wind turbines and particularly aeronautical structures. In order to reduce costs and time-consumption for in-service inspection, a number of cost effective Non-Destructive Testing (NDT) methods have been developed. The use of guided elastic waves named Lamb waves has shown promising results in detecting highly localized damages due to the relatively short wavelengths of the propagating waves in plates and shells ([1], [2]). Two common approaches for Lamb wave excitation and measurement are the pitch-catch [3] and the pulse-echo techniques. The former technique uses two transducers, one to excite the structure and the other to measure the received response. Damage is determined by characterizing the change in the response. However, in order to locate the damage, multiple pitch-catch sensors may be required. The latter technique uses one transducer to both excite the structure and detect the echoes from the excitation. The signal echoes can contribute to the determination and the localization of material defects. Focusing toward the integration of structural health monitoring in realistic applications a number of systems have been proposed. These systems are based on the development of autonomous wireless sensors and actuators which still require power supply. As a result a number of studies investigate the possibility of developing self-powered wireless health monitoring systems on vibrating structures using piezoelectric elements and electrical circuits in order to harvest electrical energy from the direct conversion of mechanical energy vibration [4].

However, the power consumption of an autonomous SHM system of aeronautical structures remains a key issue for the standard ultrasound methods used in the active approaches. An interesting alternative to

classical configurations (pitch-catch, pulse-echo) constitute the removal of the actuators and the use of a passive SHM system based on the exploitation of the ambient noise/vibration of the structures. In an aeronautical application useful noise could be the engine noise or the aerodynamic noise. Several theoretical and experimental studies have demonstrated the possibility of detecting the presence of a crack by using the ambient noise, making the assumption that a nearly spatially diffuse and temporally random acoustic field is generated in the structure. Under this assumption the Green's functions between two points of a structure can be reconstructed by the correlation of noise field recorded in these points [5].

In the aeronautical applications the acoustic vibrations produced by the engines or local aeroacoustic effects correspond to the case where the natural acoustic sources are localized rather than distributed over the structure. In this case, although the generated vibrations propagate and reverberate all over the structure, the ambient acoustic field is characterized as non-controllable, non-stationary and non-isotropic. The detection, localization and imaging of defects in such non-ideal conditions could be investigated by applying the time reversal principles associated to the singular value decomposition (DORT method) [6].

The possible non-stationarity of the ambient sources locations is a really blocking point for the application of the time reversal principles. In order to overcome this bottleneck, an innovative concept of an artificial secondary "passive" acoustic source, exploiting the contact friction nonlinearities for transferring energy from the ambient acoustic field to a secondary wave field, is proposed and fundamentally investigated in this paper.

Friction-induced vibrations [7] have been the subject of a huge amount of research works in several research fields and often aimed to their control or suppression. Sliding contacts can lead either to undesirable dynamic instabilities like macroscopic stick-slip and brake squeal [8], [9], [10], or to contact damping effects that have been largely investigated for several applications. First researches on friction damping appeared on 1931 [11], while a review on the different friction models and their applications as dampers was presented by Ferri [12] in 1995. The analysis of friction sliders as dampers needed the development of nonlinear tools for simulating and investigating the phenomena. The first studies were performed on a one degree of freedom (1DOF) model [11], while a more complex structure was modeled by Toufine et al. in 1999 [13]. Due to the huge computational effort needed for transient nonlinear simulations, several approximated methods have been proposed: e.g. the Harmonic Balanced Method [14], the Multi-Harmonic Balanced Method [15], the Incremental Harmonic Balanced Method [16], [17], [18], the Hybrid Frequency-Time domain Method [19] and the Alternative Frequency Time Domain Method [20]. The results of numerical simulations have been also compared with experimental tests on simple test benches [21]. Several works deal with friction induced vibrations itself [22] and the coupling between the system dynamics and the friction properties [23], [8], [9], [24], [25]. In these cases, finite element models of the system have been developed, including the sliding contact interfaces [25], [26], [27]. While a linear model is used for the dynamic analysis of the system, non-linear transient simulations are needed to account for the contact nonlinearities [8]. Although several works focused on contact instabilities and on the application of sliders as a damper, the specific use of friction nonlinearities as a tool for transferring energy from an acoustic field to another one at different frequencies has not yet been investigated. Recent works [28], [29], always focused on damping, deal with the energy transfer on a master / slave system to perform the transfer of the vibration energy from the structure to a set of small oscillators that are capturing energy from the mechanical system and thus are acting as nonconventional dampers.

In this context, the development of the artificial acoustic secondary source, needed for passive SHM applications, is based on a reduced multi degree-of-freedom model which is an extension of the models already investigated by the authors for the analysis of friction dampers [30].

The main idea consists in the development of a simple system constituted by a master resonator that is connected to a secondary resonator (e.g. a small beam) by a sliding surface. The vibration of the main resonator, induced by the ambient field, allows the frictional sliding at the contact surface with the secondary resonator. In such a way the vibrational energy is transferred to the secondary resonator by the random excitation at the frictional contact interface. The secondary resonator responds with its own dynamics, introducing vibrational energy in the system characterized by different frequency content (secondary acoustic field).

The paper is structured as follows: In Session 2 the concept of the energy dissipation by dry friction in a simple system is introduced, including a Masing macroslip model and taking into account the roughness of the contact surfaces. In Session 3 the concept is extended to a multi-dofs system allowing accounting for the dynamics of the primary and secondary resonator. Finally some conclusions are presented in Session 4.

2 Energy dissipation by dry friction in a 1-dof system

2.1 Mathematical modeling of contact

Devices involving dry friction [13], [31] are often used to decrease maximal amplitudes of structure response at the resonance. Each device is characterized by a different behavior depending on the geometry, as well as the position and the characteristics (dimensions, roughness, material, etc...) of the surfaces in contact. As a consequence, different adapted contact models have been developed, as presented for example in [32] - [35]. Two main categories of friction contact models are mainly encountered in nonlinear dynamics: Macroslip and Microslip [36]. The main difference between them concerns the homogeneity of their behavior along contact surfaces. Considering a Macroslip model, the behavior of the contact surface is considered global and homogeneous along the whole surface at any moment: it is either in a completely slipping or in a completely sticking state. On the other hand in Microslip models, the behavior of contact surfaces is no more homogeneous and mixed configurations may be present. Part of the contact surface may be stuck while another part may slip at the same time. Taking into account the most adapted model, a good agreement can be obtained between numerical and experimental results, as shown for example in [37] - [39]. Other approaches are developed to account for the continuous distribution of contact stresses and statii in order to investigate the role of the local contact dynamics (rupture and wave propagations) in the macroscopic frictional behavior [9], [25].

In this context, the presented approach wants to develop a simple model, implementing the Macroslip model of the contact, which is able as well to account for the vibrations induced by the frictional dry contact, accounting for surface parameters such as roughness (see section 2.2) that would generally need a full finite element discretization of the contact. The novelty of this approach is to account for the energy exchanged between surfaces and solids (through the friction induced vibrations) without modeling the contact interface, which would need prohibitive computational efforts.

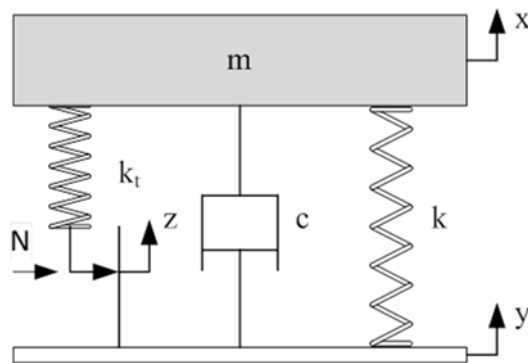


Figure 1: A spring-mass-damper-dry friction damper system

As a first step, in order to introduce the concept of energy dissipation by the dry friction, a nonlinear model of a simplified spring-mass-damper-dry friction damper system is considered (Figure 1) and the dynamic response of the system under a base excitation is analyzed. A Masing macroslip contact model is

used in order to simplify the numerical procedures and to facilitate the parametric studies. The parts in contact are either slipping or sticking. Contact separation and partial slips are not allowed.

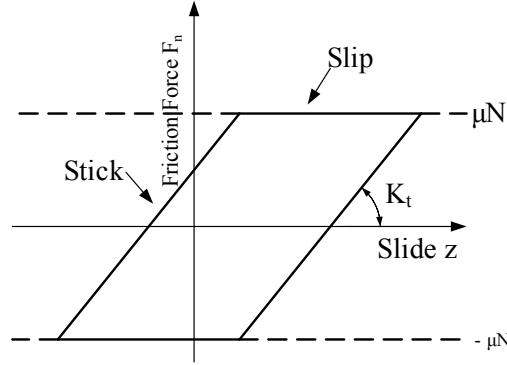


Figure 2: Hysteresis loop of the Masing model

The base of the spring-mass-damper-dry friction damper system undergoes a motion as shown at the Figure 1. Let $y(t)$ denote the absolute displacement of the base and $x(t)$ the absolute displacement of the mass from its static equilibrium position at time t . Then the net elongation of the spring is $x - y$ and the relative velocity between the ends of the damper is $\dot{x} - \dot{y}$. The governing equation of motion is:

$$m\ddot{x} + c(\dot{x} - \dot{y}) + k(x - y) + F_{NL} = 0 \quad (1)$$

where m , k , c are respectively the structural parameters mass, spring stiffness and viscous damping. F_{NL} is the nonlinear friction force due to the friction damper. N , μ and k_t represent the normal preload, the friction coefficient at the slider contact interface and the tangential stiffness of the slider in the direction of the relative motion, respectively. $w(t)$ is the displacement of the contact point with respect to the base $y(t)$ and $z(t)$ is the relative displacement between the mass and the contact point $z(t) = x(t) - y(t) - w(t)$. According to the Macroslip approach, the friction force F_{NL} can be expressed as:

$$F_{NL} = \begin{cases} k_t(x - y - z) & \text{when } k_t(x - y - z) < \mu N \\ \mu N \text{sign}(\dot{x} - \dot{y}) & \text{when } k_t(x - y - z) \geq \mu N \end{cases} \quad (2)$$

The first row of the equation corresponds to the stick case while the second row corresponds respectively to the slipping case (Figure 2). The slope of the hysteresis loop sides correspond to the stiffness of the damper. The amplitude of the friction force with respect to time t is presented in Figure 3.

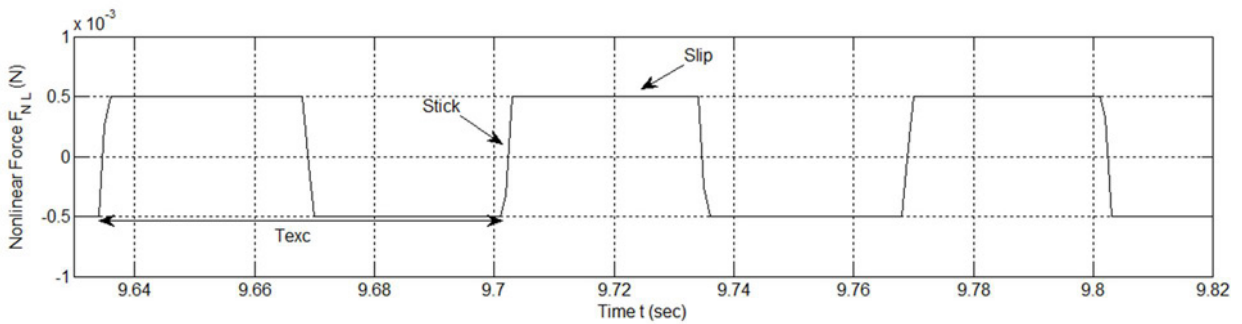


Figure 3: The friction force F_{NL} ($f_{exc}=15$ Hz, $Y=10^{-3}$ m, $N=0.001$ N)

2.2 Introduction of surface roughness

The aim of this work is to simulate the energy transfer between different acoustic fields, which is mainly due to the random excitation at the contact during dry frictional macroscopic sliding. As a result the excitation at the contact needs to be accounted for. A full finite element analysis accounting for both the system dynamics (macroscale) and the surface roughness (mesoscale) would need prohibitive computational resources. For this reason, the proposed approach wants to account for the excitation of the system dynamics, by the frictional contact, introducing a perturbative term in the friction law.

In fact, in equations (2) the surfaces are assumed perfectly rigid and smooth. In reality the contact surfaces present a roughness which influences the friction force by providing local impacts and micro-slips between the roughness plateau. Moreover, because of the compliance of the material in contact, the rupture and wave propagation at the interface originate a random excitation along the whole sliding surface. In order to introduce the local surface excitation in the contact model, a new term is added as follows:

$$F_{NL} = \begin{cases} k_t(x-y-z) & \text{when } k_t(x-y-z) < \mu N \quad \text{STICK} \\ \mu N \text{sign}(\dot{x}-\dot{y}) + c_r * |\mu N \text{sign}(\dot{x}-\dot{y})| * n & \text{when } k_t(x-y-z) \geq \mu N \quad \text{SLIP} \end{cases} \quad (3)$$

The roughness and rupture effect is added as a disturbance at the contact force during slipping. This disturbance follows a Gaussian distribution with mean value and standard deviation equal to $|\mu N \text{sign}(\dot{x}-\dot{y})|$ and $c_r * |\mu N \text{sign}(\dot{x}-\dot{y})|$ respectively. The coefficient c_r is introduced in order to quantify the extent of the roughness. In Figure 4 the shape of the hysteresis loop is presented for $c_r = 10\%$ and $c_r = 0\%$.

For this preliminary analysis, the parameters characterizing the disturbance due to the local excitation (roughness and ruptures) have been fixed with preliminary assumptions as the aim of the work is the development and analysis of the numerical model. For further analyses these parameters will be retrieved by experimental tests as a function of key parameters such as sliding velocity, normal load, material properties and surface roughness.

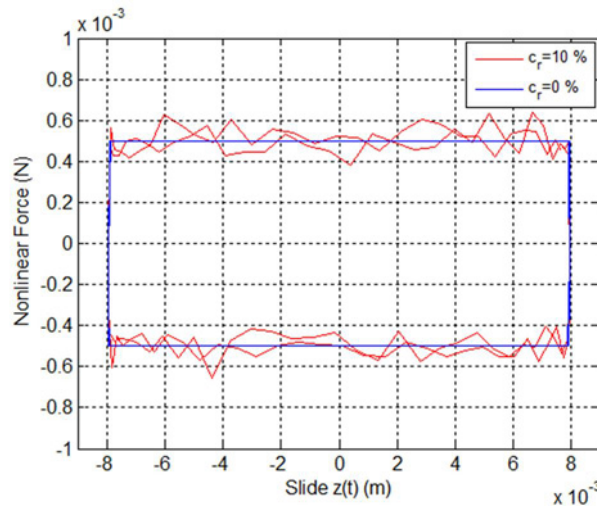


Figure 4: Shape of hysteresis loop for the roughness parameter for $c_r=0\%$ and $c_r=10\%$ ($f_{exc}=15$ Hz, $Y=10^{-3}$ m, $N=0.001$ N).

2.3 Energy balance of the system

The multiplication of the equation (1) by \dot{x} and a rearrangement of the terms lead to the expression:

$$k(y-x)\dot{y} + c(\dot{y}-\dot{x})\dot{y} = m\ddot{x} + c(\dot{x}-\dot{y})^2 + k(x-y)(\dot{x}-\dot{y}) + F_{NL}\dot{x} \quad (4)$$

The introduction of the $\dot{x} = \dot{y} + \dot{z} + \dot{w}$ and the rearrangement leads to the final equation:

$$k(y-x)\dot{y} + c(\dot{y}-\dot{x})\dot{y} - f_{NL}\dot{y} = c(\dot{x}-\dot{y})^2 + k(x-y)(\dot{x}-\dot{y}) + F_{NL}\dot{z} + F_{NL}\dot{w} + \frac{d}{dt}\left(\frac{m\dot{x}^2}{2}\right) \quad (5)$$

or

$$k(y-x)\dot{y} + c(\dot{y}-\dot{x})\dot{y} - F_{NL}\dot{y} = c(\dot{x}-\dot{y})^2 + F_{NL}\dot{z} + F_{NL}\dot{w} + \frac{d}{dt}\left(\frac{m\dot{x}^2}{2} + \frac{k(x-y)^2}{2}\right) \quad (6)$$

The equation (6) represents the power conservation of the system. In words, the instantaneous power into the system (left term) is equal to the sum of the power absorbed by the damper, the time rate increase of the sum of the kinetic and strain energies and the power absorbed by the friction damper (slider). The term $F_{NL}\dot{w}$ corresponds to the strain energy stored into the stiffness of the frictional slider, while the term $F_{NL}\dot{z}$ corresponds to the energy dissipated by the frictional slider. Part of this energy is restituted to the system by through friction induced vibrations, accounted for by the perturbative term of the frictional forces.

The prediction of the response of systems involving dry friction is complex due to its highly nonlinear behavior. In order to solve the nonlinear problem, a special technique is considered by combining a nonlinear version of Newmark integration with the Newton-Raphson iterative method. In order to perform a preliminary numerical analysis, the parameters are considered as follows: mass $m=1$ kg, system stiffness $k=10^4$ N/m and viscous damping $c=2$ Ns/m. The contact stiffness is $k_t=10^4$ N/m and the dry friction coefficient is $\mu=0.5$. A harmonic motion is applied on the base of the system: $y = y_0 \cos(2\pi f_{exc} t)$ with $y_0=10^{-4}$ m. The resulting relative displacement of the frictional slider is presented in Figure 5.

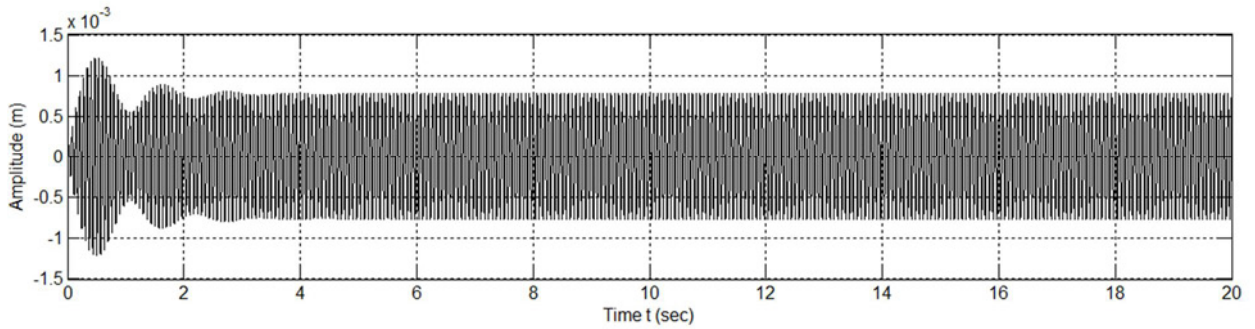


Figure 5: Dynamic response of the friction damper z for $c_r = 0\%$ and $N=0.1$ N.

The frequency response of the system is obtained for different normal loads N . For $N=0.1$ N, the contact is always sliding and the system exhibits a linear behavior. In this case, the equivalent stiffness is $k_{eq}=k$ and the resonance occurs at:

$$f_1 = \frac{1}{2\pi} \sqrt{\frac{k_{eq}}{m}} = 15.9 \text{ Hz}$$

For $N>25$ N the contact is always completely stuck and the resonant frequency is in this case a function of both system stiffness and contact stiffness. The equivalent stiffness is $k_{eq}=k+k_t$ and the resonance is at:

$$f_2 = \frac{1}{2\pi} \sqrt{\frac{k_{eq}}{m}} = \frac{1}{2\pi} \sqrt{\frac{k+k_t}{m}} = 22.5 \text{ Hz}$$

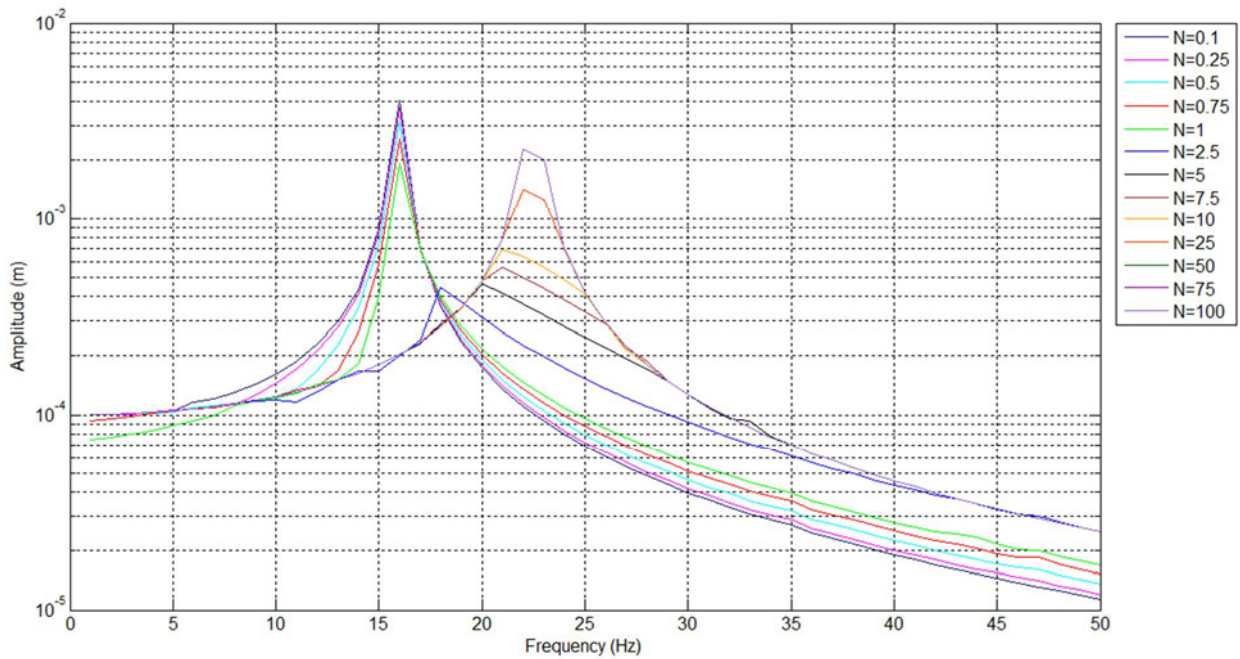


Figure 6: Amplitude of the steady state displacement calculated for different values of normal load.

When the normal load decreases from 100 N to 0.1 N, the contact state changes from stick to stick/slip state. As a consequence of those changes, peaks become flatter and the amplitudes obtained are much smaller than those associated to the linear cases when contact is completely sticking or slipping. The dynamic behavior, obtained with the single dof system with dry friction and excitation from its base, exhibits the three different contact states (stick, stick/slip, slip) and peak flattening is observed (Figure 6). An illustration of the modification of the hysteresis curves is presented in Figure 7. The case when $N=2.5$ N is very interesting as the friction damper presents a small transient displacement and sticks quickly at a non-zero position.

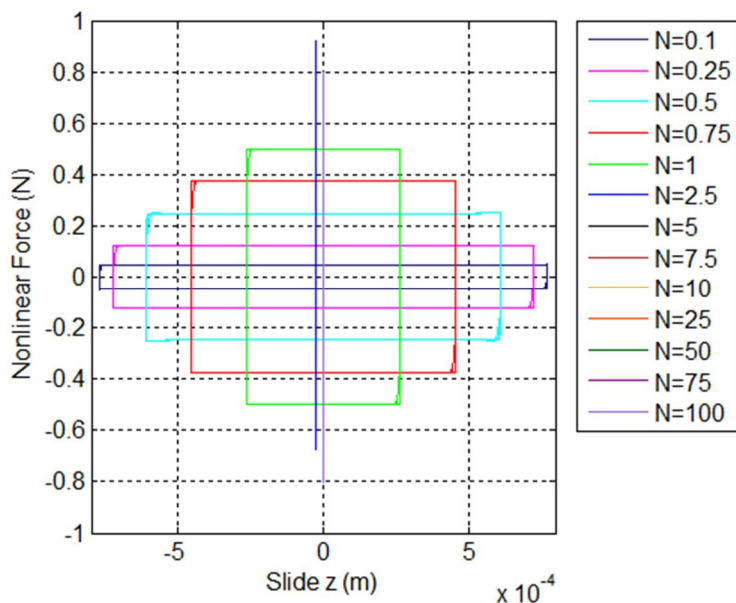


Figure 7: Shape of hysteresis loops for different normal forces N .

2.4 Estimation of the dry friction dissipated energy

The energy dissipated by the dry friction damper E_{friction} over a period of one forcing cycle may be obtained from the hysteresis loop giving the nonlinear F_{NL} as a function of the relative displacement between the mass and the contact point $z(t)$. The energy is calculated over the period of one forcing cycle at the steady state, using the expression:

$$E_{\text{friction}} = \int_T F_{\text{NL}} \dot{z} dt \quad (7)$$

The energy is calculated for different normal forces under a harmonic sweep excitation with frequency f_{exc} in the range 0-50 Hz and is normalized by the normal force. The results are presented in Figure 8. By analyzing the results, it can be concluded that a larger amount of energy is dissipated when the contact is in slipping mode.

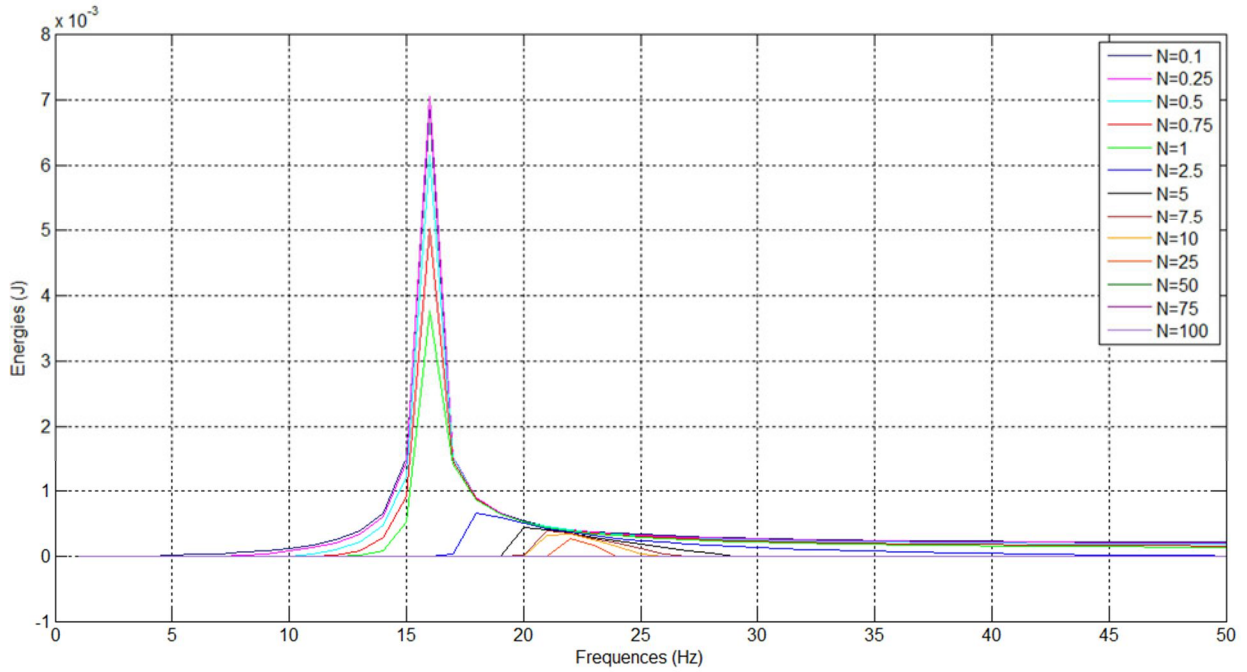


Figure 8: The energy dissipated by the dry friction damper E_{friction} for different normal forces N .

The amount of energy reintroduced as friction induced vibrations will be a percentage of the dissipated energy. For this reason, as a first approach, the sliding conditions seems to be the more appropriate to maximize the energy transfer. Nevertheless, to address this point it is necessary to account for the dynamic response of both the primary and secondary resonators, and the exchange of energy due to a slider between them. For this reason the following of the analysis is developed on a more complex model with 3 dofs.

3 Energy transfer by dry friction in a multi dofs system

3.1 Description of the 3-dofs system

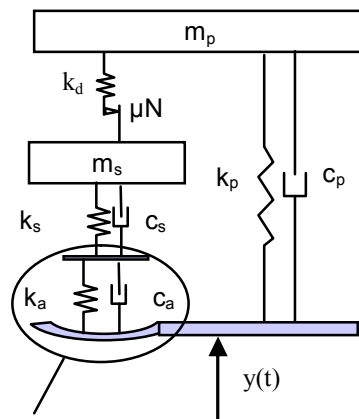
In the previous session, the concept of the energy dissipation by a dry friction damper has been presented. In this session, the concept is extended towards the vibrational energy transferred between the different natural frequencies of a system. This concept is based on the exploitation on one hand of the contact nonlinearities and on the other hand of an ambient vibroacoustic field.

A discrete system constituted by 3 degrees of freedom (3-dofs) and a frictional slider is considered, as presented in Figure 9. The two degrees of freedom (m_p & m_s) correspond to the primary resonator and the secondary resonator of the device developed for transferring the vibration energy. The third one models the local deformation of the structure (e.g. the wing local deformation in the aeronautical application). A periodic base excitation is applied on the system basement $y(t)$ simulating the ambient vibroacoustic field and a normal load is applied to the frictional slider to load the contact.

Even if the dynamics of the whole system is different from the dynamics of each component (resonators) the low coupling introduced by one point of contact (a small contact surface in the respective experimental device) allows to accept the modes of the system as modes corresponding to the natural frequency of each component; the vibration is mainly concentrated in one of the resonators. For this reason, in the following, the modes of the whole system will be referred often as modes of the primary or secondary resonators.

The working principle of the proposed device can be resumed as follows: the base excitation represents the acoustic ambient noise (e.g. vibrations coming from engines or aerodynamic noise); the principal resonator is tuned in frequency with the ambient noise such as its response to allow sliding at the slider, which connects it to the secondary resonator; the secondary resonator is excited by the frictional forces, it responds with its own dynamics and reintroduce energy into the system at its natural frequency. In such a way, the vibrational energy at the ambient acoustic frequency range (primary resonator response) is transferred to the secondary acoustic field (natural frequency of the secondary resonator).

The excitation at the contact (nonlinearity of the contact) is due partially to the slipping/sticking switches and to the perturbation introduced into the contact law, described in the previous sections.



Local deformation of structure

Figure 9: The 3 degrees of freedom (3-dofs) system

By using the Lagrange equations the system equations are formulated as follows:

$$\begin{bmatrix} m_p & 0 & 0 \\ 0 & m_s & 0 \\ 0 & 0 & m_a \end{bmatrix} \begin{bmatrix} \ddot{x}_p \\ \ddot{x}_s \\ \ddot{x}_a \end{bmatrix} + \begin{bmatrix} c_p & 0 & 0 \\ 0 & c_s & -c_s \\ 0 & -c_s & c_s + c_a \end{bmatrix} \begin{bmatrix} \dot{x}_p \\ \dot{x}_s \\ \dot{x}_a \end{bmatrix} + \begin{bmatrix} k_p & 0 & 0 \\ 0 & k_s & -k_s \\ 0 & -k_s & k_s + k_a \end{bmatrix} \begin{bmatrix} x_p \\ x_s \\ x_a \end{bmatrix} + \begin{bmatrix} -F_{nl} \\ F_{nl} \\ 0 \end{bmatrix} = \begin{bmatrix} k_p y + c_p \dot{y} \\ 0 \\ k_a y + c_a \dot{y} \end{bmatrix} \quad (8)$$

where m_i , c_i , k_i are the model parameters and F_{nl} is the nonlinear friction force.

3.2 Estimation of the energy transferred by friction induced vibrations

In order to analyze the concept of the energy transfer between the natural frequencies of the system, a multi parametrical analysis has been performed. The parameters of the system are selected such as the first natural frequency of the system (mainly related to the dynamics of the primary resonator) is tuned with the ambient acoustic field in order to maximize the vibrational response of the primary resonator. On the other hand, the second degree of freedom (mainly related with the vibrations of the secondary resonator) is tuned with the wished secondary acoustic field. The parameters and the natural frequencies of the system, defined to be representative of an experimental test bench under investigation in the framework of an ongoing project, are presented in Table 1.

Primary resonator			Secondary resonator			"Local deformation"		
f_p	68,5	Hz	f_s	946,8	Hz	f_a	68,5	Hz
m_p	0,0838	kg	m_s	0,0028	kg	m_a	1,2465	kg
k_p	15529	N/m	k_s	98059	N/m	k_a	231073	N/m
ζ	0,001		ζ	0,001		ζ	0,001	
c_p	0,072162	Ns/m	c_s	0,033314	Ns/m	c_a	1,07339	Ns/m

Table 1: Parameters of the system. The parameters are selected to be representative of an experimental test bench under investigation.

The two extreme cases, totally slip and totally stick, are firstly considered; the natural frequencies of the two corresponding systems are calculated and reported in Table 2.

Natural frequencies (Hz)			
Stick	68,5	87,3	989,8
Slip	68,5	68,4	942,9

Table 2: The natural frequencies of the two extreme cases, totally slip and totally stick

The contact stiffness is $k_t = 10^4$ N/m and the dry friction coefficient is $\mu = 0.5$. A harmonic motion is applied on the base of the system: $y = y_0 \cos(2\pi f_{exc} t)$ with $y_0 = 10^{-4}$ m and $f_{exc} = 68$ Hz (tuned with the first natural frequency of the primary resonator). The sampling frequency is selected equal to 20200 Hz. The displacement, the speed and the acceleration of each of the 3-dofs and of the frictional slider are calculated for different values of the normal load N and different values of the contact perturbation amplitude (c_r).

The power spectral density of the acceleration response of the 3-dofs, with and without the perturbative term at the contact, are estimated and presented in Figure 10, Figure 11 and Figure 12. The harmonics of the excitation frequency f_{exc} , as expected, are presented in the PSD of all the accelerations. Looking at the acceleration of the mass related to the secondary resonator (2nd dof), in Figure 11, it can be noted that the introduction of roughness leads to the identification of an excited frequency band around the natural frequency of the 2nd dof. Furthermore in Figure 12, where the PSD of the acceleration of the mass relative

to the 3rd dof is presented, the presence of a peak around the natural frequency of the 2nd dof is also detected.

This observations allows for highlighting that the friction nonlinearities, introduced by the perturbative term of the friction law (representing the local broadband excitation at the contact), provoke the transfer of energy leading to the excitation of the 2nd natural frequency of the system.

In Figure 13 the influence of the level of the introduced roughness is considered. The introduction of roughness with a low level ($c_r=10\%$) leads already to a relevant increase of frequency content of the response in the frequency band of the wished secondary acoustic field. The further increase of the roughness leads to the increase of the excitation but with a smaller increase rate.

It is worth noticing that even without the perturbative contribution a low response of the 2nd dof is observable in Figure 11. The excitation of the dynamics of the secondary resonator is probably due, in this case, to the stick-slip transitions of the slider. Nevertheless, the introduction of the perturbative term allows for clearly excite the dynamics of the secondary resonator and transfer the acoustic energy at the secondary acoustic field.

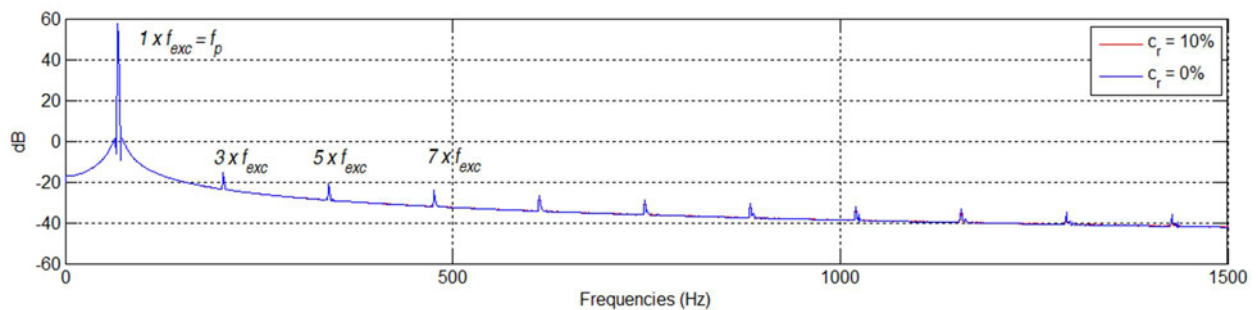


Figure 10: PSD of the acceleration of the principal resonator (1st dof) for $N=0.1$ N.

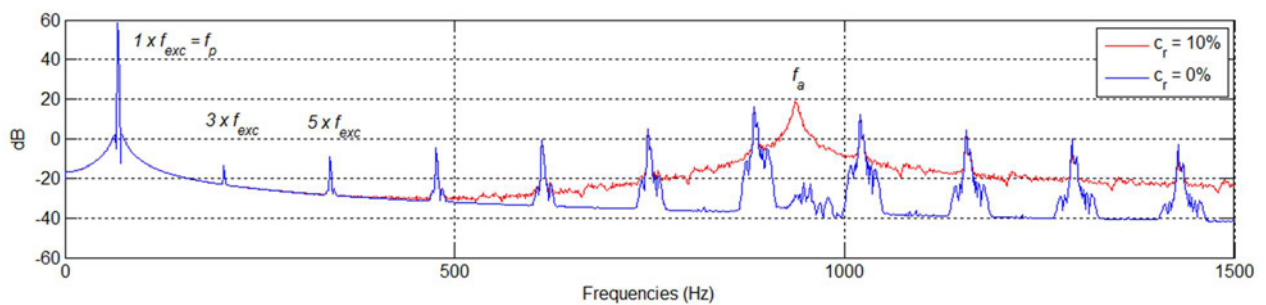


Figure 11: PSD of the acceleration of the secondary resonator (2nd dof) for $N=0.1$ N.

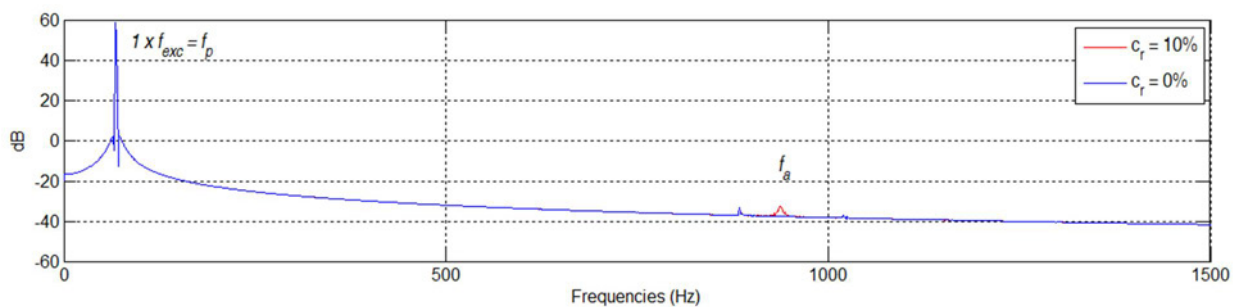


Figure 12: PSD of the acceleration of the 3rd dof (Local deformation) for $N=0.1$ N.

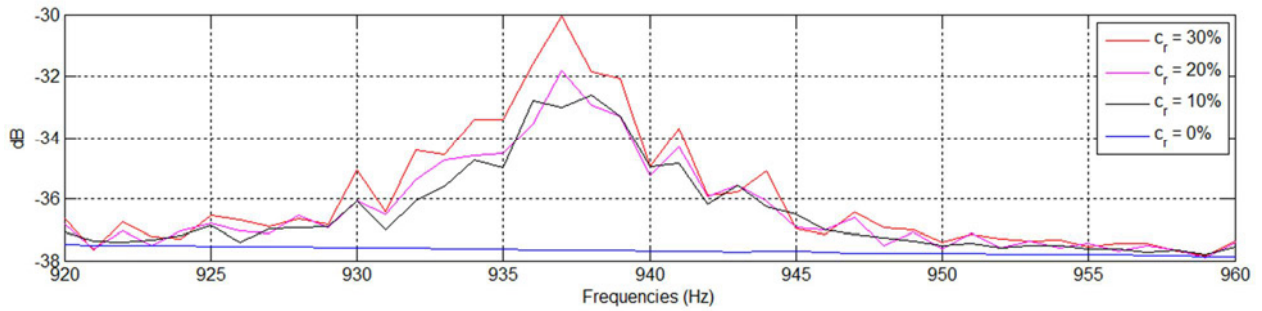


Figure 13: Zoom of the PSD of the acceleration of the 3rd dof (Local deformation) for $N=0.1$ N and four roughness levels.

4 Conclusion

A novel concept of energy transferring between acoustic fields (natural frequencies of a multi degrees of freedom system) by exploiting the dry friction nonlinearities has been proposed. The classical 1 dof model with frictional slider has been extended to a multi dof model to account for the dynamics of the single components in contact.

A 3-dofs system with excitation from the basement has been developed to introduce the ambient acoustic noise and to reproduce the dynamics of the principal and secondary resonators.

The local broadband excitation at the contact, due to roughness and ruptures at the interface, has been included in a Masing macroslip model to account for the reintroduction into the system, by friction induced vibrations, of a quota part of the energy that is associated to the sliding contact.

The numerical results show that the introduction of broadband excitation do to the sliding frictional contact contributes strongly in the transfer of energy between acoustic fields: by recovering energy from the vibration of the primary resonator, which allows for the sliding, it excites the dynamics of the secondary resonator with a different frequency content.

As a further step, the authors are working towards the experimental validation of the numerical results: by one side experiments are needed to recover reliable values of the parameters introduced into the perturbative term of the friction law; by other side ongoing experimental campaigns are aimed to reproduce the energy transfer on a test bench, which includes a transfer energy device composed by the primary and secondary resonators.

Acknowledgements

This work has been supported by the French National Research Agency (ANR): No. ANR2011 BS0903901, PASNI Project.

References

- [1] W. Luo, J. L. Rose, H. Gao, *A peak frequency shift method for guided wave thickness measurement and its realization by different transducer techniques*, in 16th WCNDT 2004-World Conference on NDT, 30 August-September 3, 2004-Montreal, Canada, 2004.
- [2] A. Pilarski, J. L. Rose, *Lamb wave mode selection concepts for interfacial weakness analysis*, *Nondestr. Eval.* 11, (1992), pp. 237–249.

- [3] J.-B. Ihn, F.-K. Chang, *Pitch-catch active sensing methods in structural health monitoring for aircraft structures*, *Struct. Health Monit.* 7, (2008), pp. 5–19.
- [4] K. Yuse, T. Monnier, L. Petit, E. Lefeuvre, C. Richard, D. Guyomar, *Self-powered Wireless Health Monitoring Supplied by Synchronized Switch Harvesting (SSH) Method*, *Journal of Intelligent Material Systems and Structures*, Vol. 19, (2008), pp. 387-394.
- [5] E. Moulin, N. A. Leyla, J. Assaad, S. Grondel, *Applicability of acoustic noise correlation for structural health monitoring in nondiffuse field conditions*, *Applied Physics Letters*, Vol. 95, 094104 (2009).
- [6] L. Chehami, E. Moulin, J. de Rosny, Cl. Prada, O. Bou Matar, F. Benmeddour, J. Assaad, *Detection and localization of a defect in a reverberant plate using acoustic field correlation*, *Journal of Applied Physics*, Vol 115, 104901 (2014).
- [7] A. Akay, *Acoustic of friction*, *Journal of Acoustical Society of America*, Vol. 111, No 4, (2002), pp. 1525-1548.
- [8] F. Massi, L. Baillet, O. Giannini, A. Sestieri, *Brake squeal phenomenon: linear and nonlinear numerical approach*, *Mechanical Systems and Signal Processing*, Vol. 21, No 6, (2007), pp. 2374-2393.
- [9] D. Tonazzi, F. Massi, A. Culla, L. Baillet, A. Fregolent, Y. Berthier, *Instability scenarios between elastic media under frictional contact*, *Mechanical Systems and Signal Processing*, Vol. 40, Issue 2, pp 754-766, 2013.
- [10] F. Cantone, F. Massi, *A numerical investigation into the squeal instability: Effect of damping*, *Mechanical Systems and Signal Processing*, Vol. 25, Issue 5, Pages 1727-1737, 2011.
- [11] J. P. Den Hartog, *Forced vibrations with combined coulomb and viscous friction*, *Transactions of the ASME*, Vol. 53, No 9, (1931), pp. 107–115.
- [12] A. A. Ferri, *Friction damping and isolation systems*, *Journal of Engineering for Gas Turbines and Power*, Vol. 117, (1995), pp. 196–206. Special 50-th Anniversary Design Issue.
- [13] A. Toufine, J. J. Barrau, M. Berthillier, *Dynamic study of a structure with flexion-torsion coupling in the presence of dry friction*, *Nonlinear Dynamics*, Vol. 18, (1999), pp. 321–337.
- [14] A. Nayfeh, D. Mook, *Nonlinear Oscillations*, John Wiley & Sons, 1979.
- [15] J. H. Wang and W. K. Chen, *Investigation of the Vibration of a Blade With Friction Damper by HBM*, *Journal of Engineering for Gas Turbines and Power*, (APRIL 1993), Vol. 115/295
- [16] S. L. Lau and Y. K. Cheung, *Amplitude incremental variational principle for nonlinear vibration of elastic systems*, *Journal of Applied Mechanics*, Vo. 48 (1981), pp. 959–964.
- [17] S. L. Lau, Y. K. Cheung, and S. Y. Wu, *Incremental harmonic balance method with multiple time scales for aperiodic vibration of nonlinear systems*, *Journal of Applied Mechanics*, Vol. 50, (1983), pp. 871–876.
- [18] S. L. Lau, W. S. Zhang, *Nonlinear vibrations of piecewise-linear systems by incremental harmonic balance method*, *Journal of Applied Mechanics*, Vol. 59, (1992), pp. 153–160.
- [19] F. H. Ling, X. X. Wu., *Fast galerkin method and its application to determine periodic solutions of non-linear oscillators*, *International Journal of Non-Linear Mechanics*, Vol. 22, No 2, (1987), pp. 89–98.
- [20] T. Cameron, J. Griffin, *An alternating frequency/time domain method for calculating the steady-state response of nonlinear dynamic systems*, *Journal of Applied Mechanics*, Vol. 56, (1989), pp. 149–154.
- [21] K.-H. Koh, J. H. Griffin, S. Filippi, A. Akay, *Characterization of turbine blade friction dampers* *Journal of engineering for gas turbines and power*, Vol. 127, No 4, (2005), pp. 856-862
- [22] G. Sheng, *Friction-induced vibrations and sound; principles and applications*, CRC / Taylor & Francis, 2008.
- [23] H. Ouyang, W. Nack, Y. Yuan and F. Chen, *Numerical analysis of automotive disk brake squeal: a review*, *Int. J. Vehicle Noise and Vibration*, Vol. 1, No. 3/4, (2005), pp. 207–231.
- [24] F. Massi, J. Rocchi, A. Culla, Y. Berthier, *Coupling system dynamics and contact behaviour: Modelling bearings subjected to environmental induced vibrations and 'false Brinelling' degradation*, *Mechanical Systems and Signal Processing*, Vol. 24, No 4, (2010), pp.1068–1080.
- [25] M. Di Bartolomeo, F. Massi, L. Baillet, A. Fregolent, Y. Berthier, A. Culla, *Wave and rupture propagation at frictional bimaterial sliding interfaces: from local to global dynamics, from stick-slip to continuous sliding*, *Tribology International*, Vol. 52, pp. 117–131, 2012.

- [26] L. Lee, G. Lou, K. Xu, , M. Matsuzaki, , B. Malott, *Direct Finite Element Analysis on Disc Brake Squeal Using the ABLE Algorithm*, SAE Paper 2003-01-3350, (2003).
- [27] J. J. Sinou, L. Jèzèquel, *Mode coupling instability in friction-induced vibrations and its dependency on system parameters including damping*, European Journal of Mechanics A / solids Vol. 26, (2007), pp. 106-122.
- [28] A. Carcaterra, A. Akay, *Theoretical Foundations of Apparent Damping Phenomena and Nearly-Irreversible Energy Exchange in Linear Conservative Systems*, J. Acoust. Soc. Amer Vol. 121, (2007), pp. 1971 – 1982.
- [29] A. Akay, Z. Xu, A. Carcaterra, I. M. Koc, *Experiment on vibration absorption using energy sinks*, J. Acoust. Soc. Amer., Vol. 118, (2005), pp. 3043 – 3049.
- [30] F. D’Ambrosio, E. Chatelet, G. Jacquet-Richardet, *Influence of contact states on the dynamic behavior of rubbing structures*, Proceedings of ASME Turbo Expo 2005, Power for Land, Sea and Air, IGTI 2005, Reno-Tahoe, Nevada USA, 06-09 June 2005, GT-2005-68560.
- [31] K. Popp, L. Panning, W. Sextro, *Vibration damping by friction forces: theory and applications*, Journal of Sound and Vibration, Vol. 9, No 3–4, (2003), pp. 419–448.
- [32] B. D. Yang, C.H. Menq, *Characterization of 3D contact kinematics and prediction of resonant response of structures having 3D frictional constraint*, Journal of Sound and Vibration, Vol. 217, No 5, (1998), pp. 909–925.
- [33] R. Masiani, D. Capecchi, F. Vestroni, *Resonant and coupled response of hysteretic two-degree-of-freedom systems using harmonic balance method*, Nonlinear Mechanics, Vol. 37, (2002), pp. 1421–1434.
- [34] K. Y. Sanliturk, D.J. Ewins, *Modelling two-dimensional friction contact and its application using harmonic balance method*, Journal of Sound and Vibration, Vol. 193, No 2, (1996), pp. 211–523.
- [35] E. P. Petrov, D.J. Ewins, *Analytical formulation of friction interface elements for analysis of nonlinear multiharmonic vibrations of bladed discs*, ASME Journal of Turbomachinery, Vol. 125, (2002), pp. 364–371.
- [36] G. Csaba, *Forced response analysis in time and frequency domains of a tuned bladed disk with friction dampers*, Journal of Sound and Vibration, Vol. 214, No 3, (1998), pp. 395–412.
- [37] L. Panning, W. Sextro, K. Popp, *Optimization of interblade friction damper design*, Proc. of 2000 ASME Turbo Expo, May 8–11, 2000, Munich, Germany 2000-GT-541, 2000.
- [38] T. Berruti, S. Filippi, M.M. Gola, S. Salvano, *Friction damping of interlocked vane segments: validation of friction model and dynamic response*, Proc. of 2002 ASME Turbo Expo, June 3–6, 2002, Amsterdam, The Netherlands, 2002-GT-30324, 2002.
- [39] E. Chatelet, G. Michon, L. Manin, G. Jacquet, *Stick/slip phenomena in dynamics: choice of contact model. Numerical predictions & experiments*, Journal of Mechanism and Machine Theory, Vol. 43, (2008), pp. 1211–1224.